

Analysis and Optimization of Laminated Circular Cylindrical Shell

EVA KORMANÍKOVÁ, KAMILA KOTRASOVÁ

Institute of Structural Engineering

Civil Engineering Faculty, Technical University of Košice

Vysokoškolská 4, 042 00 Košice

SLOVAKIA

eva.kormanikova@tuke.sk, kamila.kotrasova@tuke.sk

Abstract: - Structural optimization using computational tools has become a major research field in recent years. The paper deals with a sizing optimization analysis of laminated circular cylindrical shell. For thin-walled shells, the classical shell theory is capable of accurately predicting the shell behavior. The weight minimization subjected to displacement constraint within the numerical optimization of the circular cylindrical shell is done. The thickness of the shell laminate roof under constant pressure loading is being searched in the optimization process. The boundary conditions of the shell laminate roof are assumed to be a fully pin support. Within the general optimization process, the Modified Feasible Direction method is used. The performance of the composite structural system is evaluated through finite element analysis of shell elements carried out using COSMOS/M.

Key-Words: - laminate composite, homogenization, circular cylindrical shell, classical shell theory, sizing optimization

1 Introduction

Structural designers seek the best possible design, be it a vehicle structure or space structure while using the least amount of resources. The quality of a design depends on the application, typically related to strength or stiffness, while resources are measured in terms of weight or cost. Therefore, the best design often means the lowest weight or cost with limitations on the strength or stiffness properties. Engineers have relied on experience to achieve such design.

Over past decades, mathematical optimization, which deals with either the maximization or minimization of an objective function subject to constraint functions, has emerged as a powerful tool for structural design. The use of mathematical optimization of design transforms the design process into a systematic well-organized activity.

For many years, designers have investigated optimization problems involving composite materials. Using composite materials in structural design [1,2] has gained popularity, because of several advantages that these materials offer. The directionality of fiber composites requires the optimization in the process of design of these materials. Many works have been done on optimization of cylindrical shells, for example, Park et al. [3] used optimization of laminate stacking sequence to maximize the strength. Adali and Verijenko [4] optimized the stacking sequence

design for hybrid laminates. Soremekun et al. [5] used optimization algorithm for stacking sequence blending of multiple composite laminates to minimize the weight and the cost of the panels. Weaver [6] used computational study for designing the laminate composite cylindrical shells under axial compression to minimize the mass with local and global constraints.

Many works have treated the optimization of circular cylindrical shells. Lam and Loy [7] investigated the influence of boundary conditions for rotating cylindrical shell made of thin laminate. Duvaut et al. [8] developed a finite element method for determining the optimal direction and the fiber volume fraction at each point of a structure to minimize the weight. Numerical simulation of fiber reinforced composites has been done in 3D [9]. Hu and Ou [10] used a sequential linear programming method (SLP) for the maximization of the fundamental frequency of truncated conical laminated shells with respect to the orientations of fibers.

The paper is organized as follows. In Section 2 the Mori-Tanaka (MT) method [11] is expressed, that has applications in a variety of engineering works. The classical theory for a circular cylindrical shell [12] using Love's first approximation is discussed in Section 3. In Section 4 we introduced the Finite Element Method (FEM) [13,14,15] into the problem. The Sizing Optimization Problem [16] as an iterative

process of engineering design is given in Section 5. Homogenization of fiber reinforced composite material [17,18,19] and Optimization [20,21,22,23, 24] of the shell roof fabricated from fiber reinforced composite laminate is explained in Section 6. Finally, we have collected some concluding remarks in Section 7.

2 Mori-Tanaka method

As an alternative to the experimental determination of material properties of fiber matrix composite material is the usage of various homogenization techniques. Many analytical homogenization techniques are based on the equivalent eigenstrain method, which considers the problem of a single inclusion embedded in an infinite elastic medium. Homogenization has been accomplished by using various techniques including the Fourier series technique, variational principles etc. Most fiber matrix composites have a random arrangement of the fibers (Fig. 1).

In the last decade, effective media theories, widely used in classical continuum micro mechanics, have been recognized as an attractive alternative to FE based methods. Since its introduction, the Mori-Tanaka method has enjoyed a considerable interest in a variety of engineering applications. These include classical fiber matrix composites too [11].



Fig. 1 Randomly distributed fibers

General description of the Mori-Tanaka method in the framework of elasticity is treated in this section. The Mori-Tanaka method takes into account the effect of phase interactions on the local stresses by assuming an approximation in which the stress in each phase is equal to that of a single inclusion embedded into an unbounded matrix subjected to as yet unknown average matrix strain or stress.

The constitutive equation $\sigma = C\varepsilon$ we can write in the following form:

$$\begin{Bmatrix} \sigma_1 \\ \sigma_2 \\ \sigma_3 \\ \sigma_4 \\ \sigma_5 \\ \sigma_6 \end{Bmatrix} = \begin{bmatrix} n & l & l & 0 & 0 & 0 \\ l & (k+m) & (k-m) & 0 & 0 & 0 \\ l & (k-m) & (k+m) & 0 & 0 & 0 \\ 0 & 0 & 0 & m & 0 & 0 \\ 0 & 0 & 0 & 0 & p & 0 \\ 0 & 0 & 0 & 0 & 0 & p \end{bmatrix} \begin{Bmatrix} \varepsilon_1 \\ \varepsilon_2 \\ \varepsilon_3 \\ \varepsilon_4 \\ \varepsilon_5 \\ \varepsilon_6 \end{Bmatrix}. \quad (1)$$

Material characteristics we can solve from the following equations

$$\begin{aligned} k &= -\left(1/G_{23} - 4/E_{22} + 4\nu_{12}^2/E_{11}\right)^{-1}, \quad l = 2k\nu_{12}, \\ m &= G_{23}, \\ n &= E_{11} + 4k\nu_{12}^2 = E_{11} + l^2/k, \quad p = G_{12}. \end{aligned} \quad (2)$$

3 Classical Shell Theory

Thin-walled laminate shells can be also modeled as two-dimensional structural elements but with single or double curved reference surfaces (Fig. 2).

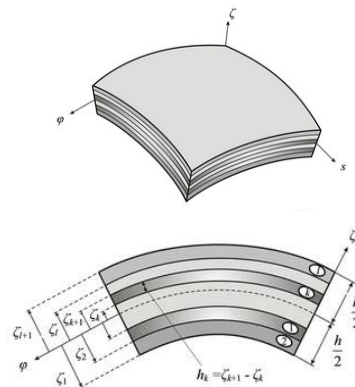


Fig. 2 Double curved laminated shell and layout of layers [25]

The modeling and analysis of laminate circular cylindrical shells fabricated from fiber composite material depend on the radius/thickness ratio (Fig. 3).

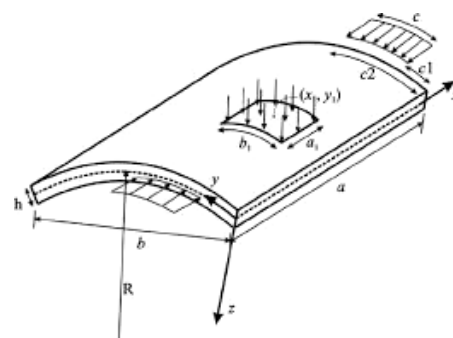


Fig. 3 Circular cylindrical shell under general loading [26]

The strain displacement relations for a circular cylindrical shell using Love's first approximation are given by

$$\begin{aligned} \bar{\varepsilon}_x &= \frac{\partial u}{\partial x}, \\ \bar{\varepsilon}_s &= \frac{\partial v}{\partial s} + \frac{w}{R}, \quad \bar{\varepsilon}_{xs} = \frac{\partial u}{\partial s} + \frac{\partial v}{\partial x}, \\ \kappa_x &= -\frac{\partial^2 w}{\partial x^2}, \quad \kappa_s = -\frac{\partial^2 w}{\partial s^2} + \frac{1}{R} \frac{\partial v}{\partial s}, \\ \kappa_{xs} &= -2 \frac{\partial^2 w}{\partial x \partial s} + \frac{1}{R} \frac{\partial v}{\partial x}. \end{aligned} \quad (1)$$

The total strains at an arbitrary distance z of the middle surface are written by

$$\begin{aligned} \varepsilon_x &= \bar{\varepsilon}_x + \kappa_x z, \\ \varepsilon_s &= \bar{\varepsilon}_s + \kappa_s z, \\ \varepsilon_{xs} &= \bar{\varepsilon}_{xs} + \kappa_{xs} z. \end{aligned} \quad (2)$$

Each individual layer is assumed to be in a state of generalized plane stress, the Hooke's law yields

$${}^n \sigma_i = {}^n E_{ij} \varepsilon_j, \quad i, j = (x, s, xs), \quad (3)$$

where n is a number of one layer and E_{ij} is a component of elasticity matrix defined in [12]. The force and moment resultants (Fig. 4) are defined by

$$N_i = \int_{-h/2}^{h/2} \sigma_i dz, \quad M_i = \int_{-h/2}^{h/2} \sigma_i z dz, \quad i, j = (x, s, xs). \quad (4)$$

The constitutive equations are written in the matrix form

$$\begin{pmatrix} \mathbf{N} \\ \mathbf{M} \end{pmatrix} = \begin{pmatrix} \mathbf{A} & \mathbf{B} \\ \mathbf{B} & \mathbf{D} \end{pmatrix} \begin{pmatrix} \bar{\boldsymbol{\varepsilon}} \\ \boldsymbol{\kappa} \end{pmatrix}, \quad (5)$$

where \mathbf{A} is the extension matrix, \mathbf{B} is the bending-extension coupling matrix, \mathbf{D} is the bending matrix. The components of \mathbf{A} , \mathbf{B} , \mathbf{D} matrix are

$$\begin{aligned} A_{ij} &= \sum_{n=1}^N {}^n E_{ij} ({}^n z^{-n-1} z), \quad B_{ij} = \frac{1}{2} \sum_{n=1}^N {}^n E_{ij} ({}^n z^2 - {}^{n-1} z^2), \\ D_{ij} &= \frac{1}{3} \sum_{n=1}^N {}^n E_{ij} ({}^n z^3 - {}^{n-1} z^3) \end{aligned} \quad (6)$$

where N stands for number of layers. The equilibrium equations for differential shell element on Fig. 4 are given by

$$\begin{aligned} \frac{\partial N_x}{\partial x} + \frac{\partial N_{xs}}{\partial s} &= -p_x, \\ \frac{\partial N_{xs}}{\partial x} + \frac{\partial N_s}{\partial s} + \frac{1}{R} \left(\frac{\partial M_s}{\partial s} + \frac{\partial M_{xs}}{\partial x} \right) &= -p_s, \\ \frac{\partial^2 M_x}{\partial x^2} + 2 \frac{\partial^2 M_{xs}}{\partial x \partial s} + \frac{\partial^2 M_s}{\partial s^2} - \frac{N_s}{R} &= -p_z. \end{aligned} \quad (7)$$

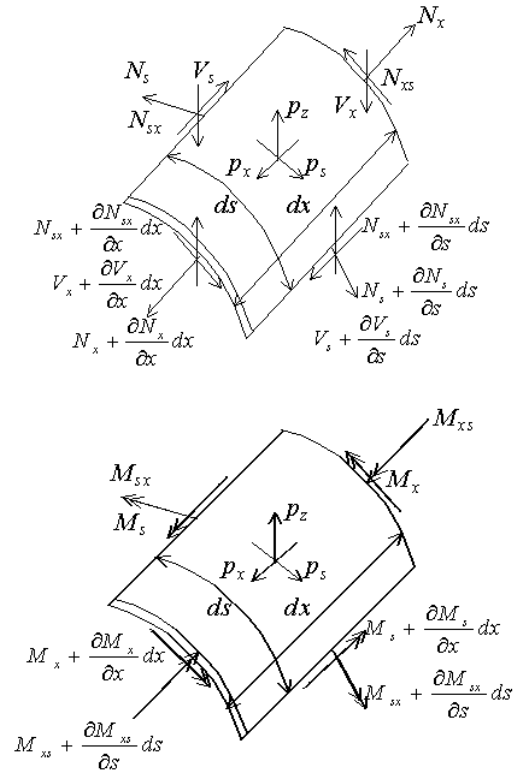


Fig. 4 Force and bending moment resultants of the differential shell element

Substituting the constitutive equations into the equilibrium equations yields a set of three coupled partial differential equations for the three displacements u, v, w which can be written in matrix form

$$\begin{pmatrix} L_{11} & L_{12} & L_{13} \\ L_{21} & L_{22} & L_{23} \\ L_{31} & L_{32} & L_{33} \end{pmatrix} \begin{pmatrix} u \\ v \\ w \end{pmatrix} = - \begin{pmatrix} p_x \\ p_s \\ p_z \end{pmatrix}, \quad (8)$$

where

$$L_{11} = A_{11} \frac{\partial^2}{\partial x^2} + 2A_{16} \frac{\partial^2}{\partial x \partial s} + A_{66} \frac{\partial^2}{\partial s^2},$$

$$L_{12} = (A_{16} + R^{-1} B_{16}) \frac{\partial^2}{\partial x^2}$$

$$+ \left(A_{12} + R^{-1} B_{12} + A_{66} + R^{-1} B_{66} \right) \frac{\partial^2}{\partial x \partial s} \\ + \left(A_{26} + R^{-1} B_{26} \right) \frac{\partial^2}{\partial s^2},$$

$$L_{13} = R^{-1} A_{16} \frac{\partial}{\partial x} + R^{-1} A_{26} \frac{\partial}{\partial s} - B_{11} \frac{\partial^3}{\partial x^3} \\ - 3B_{16} \frac{\partial^3}{\partial x^2 \partial s} - (B_{12} + B_{66}) \frac{\partial^3}{\partial x \partial s^2} - B_{26} \frac{\partial^3}{\partial s^3},$$

$$L_{22} = \left(A_{66} + 2R^{-1} B_{66} + R^{-2} D_{66} \right) \frac{\partial^2}{\partial x^2} \\ + 2 \left(A_{26} + 2R^{-1} B_{26} + 2R^{-2} D_{26} \right) \frac{\partial^2}{\partial x \partial s} \\ + \left(A_{22} + 2R^{-1} B_{22} + R^{-2} D_{22} \right) \frac{\partial^2}{\partial s^2},$$

$$L_{23} = R^{-1} \left(A_{26} + R^{-1} B_{26} \right) \frac{\partial}{\partial x} + R^{-1} \left(A_{22} + R^{-1} B_{22} \right) \frac{\partial}{\partial s} \\ - \left(B_{16} + R^{-1} D_{16} \right) \frac{\partial^3}{\partial x^3} \\ - \left(B_{12} + 2B_{66} + R^{-1} (D_{12} + 2D_{66}) \right) \frac{\partial^3}{\partial x^2 \partial s} \\ - 3 \left(B_{26} + R^{-1} D_{26} \right) \frac{\partial^3}{\partial x \partial s^2} - \left(B_{22} + R^{-1} D_{22} \right) \frac{\partial^3}{\partial s^3},$$

$$L_{33} = R^{-2} \left(A_{22} + R^{-1} B_{22} \right) + 2R^{-1} B_{12} \frac{\partial^2}{\partial x^2} + 4R^{-1} B_{26} \frac{\partial^2}{\partial x \partial s} \\ + 2R^{-1} B_{22} \frac{\partial^2}{\partial s^2} \\ - D_{11} \frac{\partial^4}{\partial x^4} - 4D_{16} \frac{\partial^4}{\partial x^3 \partial s} - 2(D_{12} + 2D_{66}) \frac{\partial^4}{\partial x^2 \partial s^2} \\ - 4D_{26} \frac{\partial^4}{\partial x \partial s^3} - D_{22} \frac{\partial^4}{\partial s^4}.$$

The governing equations are solved with the help of Finite Element Method.

4 Finite Element Analysis

The basic idea of the FEM is a discretisation of the continuous structure. The discretisation is defined by a finite element mesh made out of elements nodes. The starting point for elastostatic problems is the total potential energy. In accordance with the Ritz method, the approximation is used for displacement field vector by notation

$$\tilde{u}(x) = N(x)v, \quad (9)$$

where $N(x)$ is the matrix of the shape functions, that are functions of the position vector $x = (x, s, z)$ and v is the element displacement vector.

For the stresses and strains, we obtain from Eq. (9) the Eqs. (10)

$$\sigma(x) = E\varepsilon(x) = EDN(x)v,$$

$$\varepsilon(x) = Du(x) = DN(x)v = B(x)v. \quad (10)$$

With the approximation (Eq. 9) the total potential energy is a function of all the nodal displacement components arranged in the element displacement vector v . The variation of the total potential energy

$$\delta\Pi = \delta v^T \left(\int_V B^T E B v dV - \int_V N^T p dV - \int_{O_q} N^T q dO \right) \quad (11)$$

leads to

$$\delta v^T (Kv - f_p - f_q) = 0, \quad (12)$$

where p , q are volume and surface loadings, respectively and K is the symmetric stiffness matrix given by

$$K = \int_V B^T E B dV. \quad (13)$$

The vectors of the volume and the surface forces are written by

$$f_p = \int_V N^T p dV,$$

$$f_q = \int_{O_q} N^T q dO. \quad (14)$$

If the components of δv are independent of each other, we obtain from Eq. (12) the system of linear equations

$$Kv = f,$$

$$f = f_p + f_q. \quad (15)$$

All equations considered above are valid for a single finite element and they should have an additional index E . We have the inner element energy

$$U_E = \frac{1}{2} v_E^T \int_{V_E} B^T E B dV v_E = \frac{1}{2} v_E^T K_E v_E, \quad (16)$$

with the element stiffness matrix

$$K_E = \int_{V_E} B^T E B dV,$$

$$E = \sum_{n=1}^N {}^n E,$$

$${}^n E = \bar{T}^T ({}^n \beta) ({}^n) E_L \bar{T} ({}^n \beta), \quad (17)$$

where E is the elasticity matrix obtained with suitable transformations in two stages, firstly from the principal material directions to the element local directions and secondly to the global directions. B is the strain matrix, β is fiber orientation angle of layer, T is the transformation matrix with

$$\bar{T}(\beta) = (T^T(\beta))^{-1}. \quad (18)$$

Because the energy is a scalar quantity, the potential energy of the whole structure can be obtained by summing the energies of single elements. By a Boolean matrix L_E the correct position of each single element is determined. The element displacement vector v_E is positioned into the system displacement vector by the equation

$$v_E = L_E v, \quad (19)$$

then we obtain the system equation by summing over all elements [13]

$$\left(\sum_i L_{iE}^T K_{iE} L_{iE} \right) v = \left[\sum_i L_{iE} (f_{iEp} + f_{iEq}) \right]. \quad (20)$$

The system stiffness matrix is also symmetric, but it is a singular matrix. After consideration of the boundary conditions of the whole system, K becomes a positive definite matrix and the system equations can be solved.

5 Sizing Optimization Problem

Engineering design is an iterative process. The design is continuously modified until it meets evaluation and acceptance criteria set by the engineer.

Design optimization refers to the automated redesign process that attempts to minimize an objective function subject to limits or constraints on the response by using a rational mathematical approach to yield improved designs.

An optimum design is defined as a point in the design space for which the objective function is minimized or maximized and the design is feasible. The basic problem is the minimization of a function subject to inequality constraints:

Minimize objective function

$$Z = F(X) \rightarrow \min, \quad (21)$$

subject to constraints

$$\bar{X}_i^L \leq X_i \leq \bar{X}_i^U \quad i = 1, 2, \dots, N_d, \quad (22)$$

$$g_j(X) \leq 0 \quad j = 1, 2, \dots, N_c, \quad (23)$$

where X_i is a design variable.

We make use of the existing response at a number of points in the design space to construct a polynomial approximation to the response at other points. The optimization process is applied to the approximate problem represented by the polynomial approximation

$$F = a_0 + \sum_{i=1}^{N_d} a_i X_i + \sum_{i=1}^{N_d} b_i X_i^2 + \sum_{i=1}^{N_d-1} \sum_{j=i+1}^{N_d} c_{ij} X_i X_j + \sum_{i=1}^{N_d} d_i X_i^3 \quad (24)$$

where N_d is the number of design variables, a_i, b_i, c_{ij}, d_i are coefficients to be determined by the least squares regression.

When the objective function and constraints are approximated and their gradients with respect to the design variables are calculated based on chosen approximation, it is possible to solve the approximate optimization problem.

One of the algorithms used in the optimization module is called the Modified Feasible Direction method (MFD). The solving process is iterated until convergence is achieved.

Figure 5 shows the iterative process within the general optimization.

Using the MFD the solving process is iterated until convergence is achieved:

1. $q = 0, X^q = X^m$.
2. $q = q + 1$.
3. Evaluate objective function and constraints.
4. Identify critical and potentially critical constraints \bar{N}_c .
5. Calculate gradient of objective function $\nabla F(X_i)$ and constraints $\nabla g_k(X_i)$, where $k = 1, 2, \dots, \bar{N}_c$.
6. Find a usable-feasible search direction S^q .
7. Perform a one-dimensional search $X^q = X^{q-1} + \alpha S^q$.
8. Check convergence. If satisfied, make $X^{m+1} = X^q$. Otherwise, go to 2.
9. $X^{m+1} = X^q$.

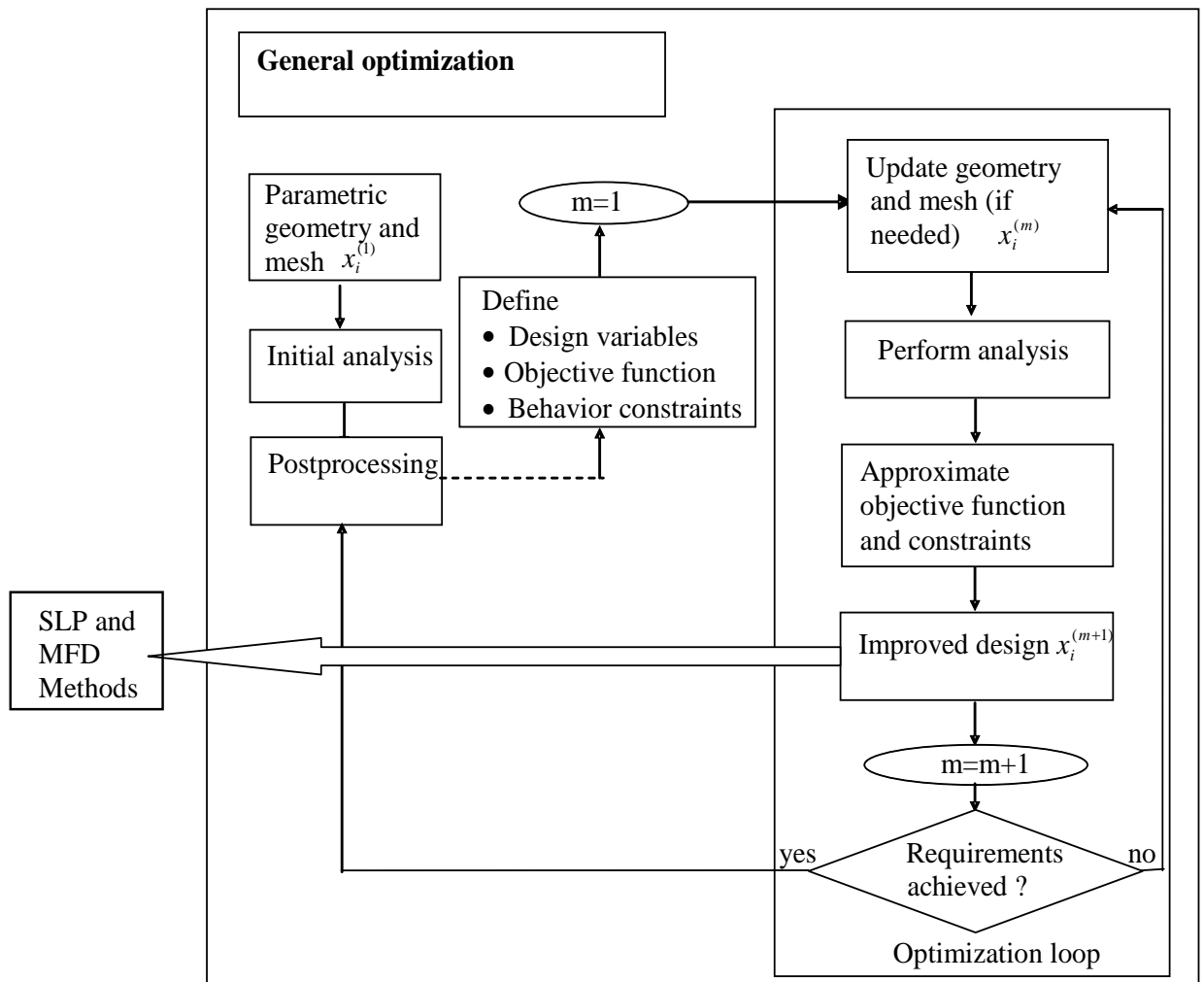


Fig. 5 General optimization process

6 Optimization Example and Results

The optimal thickness design of circular cylindrical shell fabricated from laminate $[0/45/-45/90]_S$ under constant pressure loading p_z is solved in the example (Fig. 6). The boundary conditions are assumed to be a fully pin support.

The material characteristics are computed for a unidirectional composite with isotropic fibers $E_f = 230$ GPa, $\nu_f = 0.3$, and isotropic matrix $E_m = 3.2$ GPa, $\nu_m = 0.4$. The material properties of each layer were used from homogenization techniques [11]. The fiber volume fraction and fiber diameter were found from the electron microscope digital shot (Fig. 7). Each layer of the laminate has the same thickness ${}^n h$. Initial values and results of the optimization process are listed in Table 1.

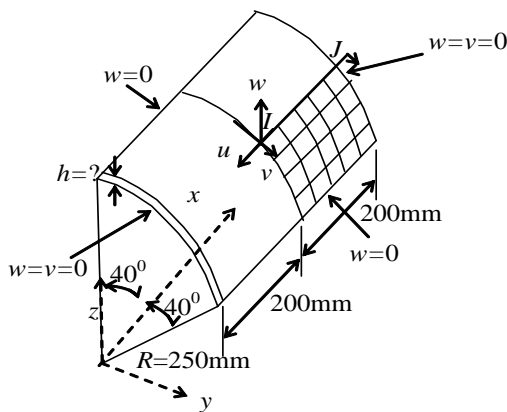


Fig. 6 Problem sketch and finite element model

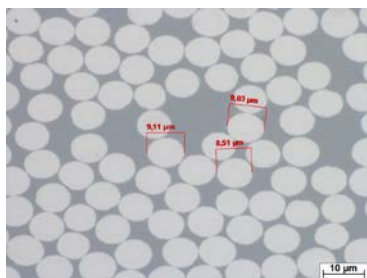


Fig. 7 Electron microscope digital shot

The mathematical optimization problem can be written as:

Minimize objective function

$$F(\mathbf{X}) = G({}^n h) \rightarrow \min \quad [\text{N}]$$

Subject to constraints

$$0.0125 \leq {}^n h \leq 0.625 \quad [\text{mm}]$$

$$-3.0 \leq w({}^n h) \leq 0.0 \quad [\text{mm}] \quad (25)$$

where ${}^n h$ is the thickness of one layer.

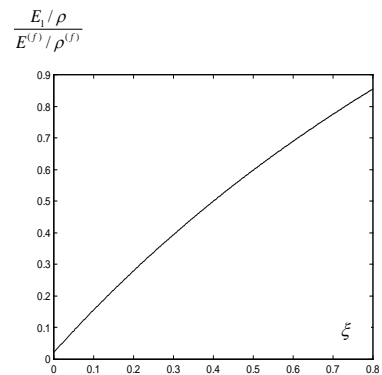


Fig. 8 Normalized longitudinal modulus versus fiber volume fraction

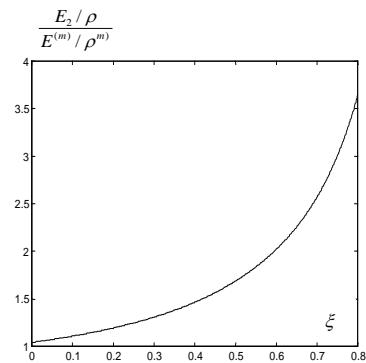


Fig. 9 Normalized transversal modulus versus fiber volume fraction

Table 1 Initial and final values of optimization parameters

Optimization parameters	Initial values	Final values	Tolerance
Design variables - thickness of one layer [mm]	0.25	0.1619	$1 \cdot 10^{-3}$
Objective function - weight [N]	4.4064	2.8532	0.01
Constraint - displacement w [mm]	-1.2478	-3.0296	0.03

Using the MFD the solving process is iterated until convergence is achieved. To find the search direction, active and violated constraints have to be identified.

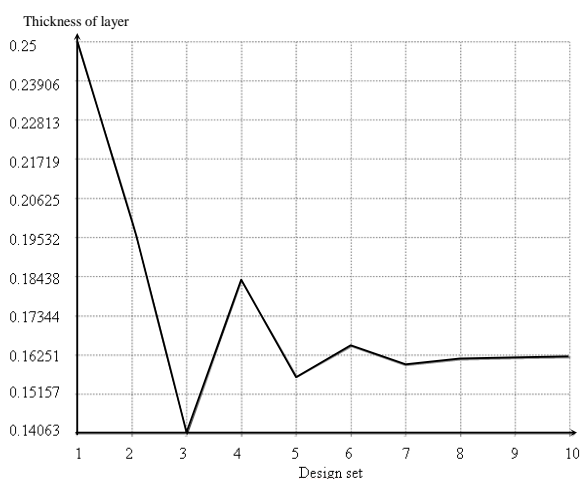


Fig. 10 Variation of the design variable values – thickness [mm] during the optimization process

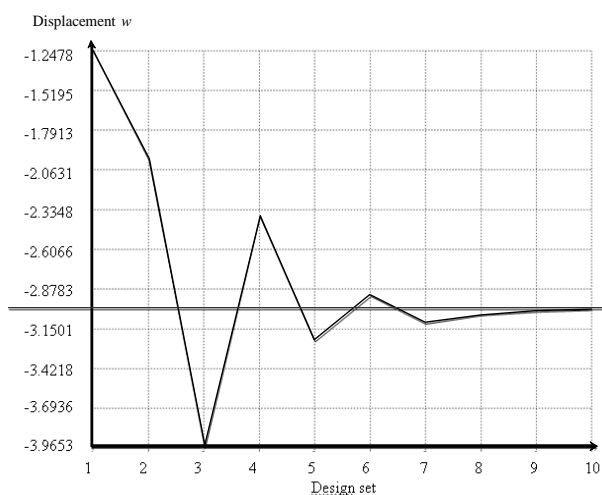


Fig. 11 Variation of the constraint values – displacement w [mm] during the optimization process

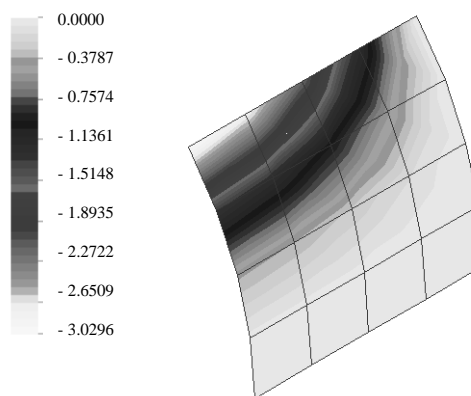


Fig. 12 Displacements w [mm] after optimization process

Convergence to the optimum is checked by criteria of maximum iterations and criteria changes of objective function. Besides these criteria, the Kuhn-Tucker conditions necessary for optimality must be satisfied by using the Lagrangian multiplier method. The Kuhn-Tucker conditions are sufficient for optimality when the number of active constraints is equal to the number of design variables and if objective function and all of the constraints are convex. Otherwise, sufficient conditions require the second derivatives of the objective function and constraints. Convergence or termination checks are performed at the end of each optimization loop. The optimization process continues until either convergence or termination occurs.

The general optimization contains:

1. Initial analysis with input data (Tab. 1).
2. Mathematical optimization problem (25).
3. Linear approximation problem.
4. The algorithm of MFD method with convergence criteria.
5. Convergence or termination checks of general optimization.

7 Concluding Remarks

The proceeding deals with a numerical approach of modeling of circular cylindrical shell fabricated from fiber reinforced composite material. The theory of cylindrical shells is described in the frame of classical shell theory. In the paper, there are involved the strain displacement relations, constitutive equations, and differential equilibrium equations.

The homogenization of fiber reinforced composite (Fig. 7) was used for calculating the material characteristics of the composite. In the Figs. 8 and 9 can be seen normalized longitudinal and transversal material modulus versus fiber volume fraction, respectively.

Within the numerical optimization, the minimization of weight subject to displacement constraint was made. Design variable is the thickness of layers of laminate cylindrical shell. The initial and final values of design variables, constraints and the objective function are shown in Table 1.

The maximum number of iterations of MFD was 100. The general optimization process was stopped after 10 design sets (Fig. 10, Fig. 11), because the difference between the current value and the one or two previous designs was less than tolerance specified in Table 1.

The final value of design variable is $h = 0.16187$ mm (Fig. 10). The total thickness of the laminate circular cylindrical shell is $8h = 1.3$ mm. Figure 11 shows the feasible and infeasible domain in the usable design space. Contour plot of displacements w after optimization process can be seen in Fig. 12.

The optimization is a very useful way for the design of laminate structural elements including circular cylindrical shells.

Acknowledgment:

This work was supported by the Scientific Grant Agency of the Ministry of Education of Slovak Republic and the Slovak Academy of Sciences under Projects VEGA 1/0477/15 and 1/0078/16.

References:

- [1] M. Zmindak, Z. Pelagic, M. Bvoc, Analysis of high velocity impact on composite structures, *Appl. Mech. and Mat.* 617, p. 104-109, 2014.
- [2] M. Major, K. Kuliński, I. Major, Thermal and Dynamic Numerical Analysis of a Prefabricated Wall Construction Composite Element Made of Concrete-polyurethane. *Procedia Engineering* (Amsterdam, Elsevier). 190, pp. 231-236, 2017.
- [3] JH. Park, JH. Hwang, CS. Lee, W. Hwang, Stacking sequence design of composite laminated for maximum strength using genetic algorithms, *Compos Struct* 52, p. 217–31, 2001.
- [4] S. Adali, V. Verijenko, Optimum stacking sequence design of symmetric hybrid laminates undergoing free vibration. *Compos Struct* 54, p. 131–8, 2001.
- [5] G. Soremekun, Z. Gurdal, C. Kassapoglou, D. Toni, Stacking sequence blending of multiple composite laminates using genetic algorithms, *Compos Struct*, 56, p. 53–62, 2002.
- [6] PM. Weaver, Design of laminated composite cylindrical shells under axial compression. *Composites Part B* 31, p. 669–79, 2000.
- [7] KY. Lam, CT. Loy, Influence of boundary conditions for a thin laminated rotating cylindrical shell. *Compos Struct*, 41:215–28, 1998.
- [8] G. Duvaut, G. Terrel, F. Lene, Verijenko VE, Optimization of fibre reinforced composites. *Compos Struct*, 48:83–9, 2001.
- [9] M. Žmindák, P. Novák, R. Melicher, Numerical simulation of 3D elastoplastic inclusion problems using boundary meshless methods, In: *Mechanics of composites materials and structures*, p. 32 – 43, 2008.
- [10] H. Hu, SC. Ou, Maximization of the fundamental frequencies of laminated truncated conical shells with respect to fibre orientations. *Compos Struct*, 52:265–75, 2001.
- [11] J. Vorel, M. Šejnoha, *Documentation for HELP program, Theoretical manual and user guide*, Czech Technical University in Prague, Faculty of Civil Engineering, 2008.
- [12] H. Altenbach, J. Altenbach, W. Kissing, *Structural analysis of laminate and sandwich beams and plates*. Lubelskie Towarzystwo Naukowe, Lublin, 2001.
- [13] E. J. Barbero, *Finite Element Analysis of Composite Materials*. CRC Press, Taylor & Francis Group, 2008.
- [14] J. Melcer, G. Lajcakova, Comparison of finite element and classical computing models of reinforcement pavement, *Adv. Mat. Res.* 969, p. 85-88, 2014.
- [15] E. Kormanikova, I. Mamuzic, Optimization of laminates subjected to failure criterion, *Metal*. 50 (1), p. 41-44, 2011.
- [16] E. Kormanikova, K. Kotrasova, Sizing optimization of sandwich plate with laminate faces, *International Journal of Mathematics and Computers in Simulation*, Volume 10, Pages 273-280, 2016.
- [17] M. Sejnoha, J. Zeman, Micromechanical modeling of imperfect textile composites, *Int. Jour. of Eng. Scien.* 46 (6), p. 513-526, 2008.
- [18] J. Ma, S. Sahraee, P. Wriggers, L. De Lorenzis, Stochastic multiscale homogenization analysis of heterogeneous materials under finite deformations with full uncertainty in the microstructure, *Comp. Mech.* 55, Issue 5, p. 819-835, 2015.
- [19] C. Maruccio, L. De Lorenzis, L. Persano, D. Pisignano, Computational homogenization of fibrous piezoelectric materials, *Comp. Mech.* 55, Issue 5, p. 983-998, 2015.
- [20] M. Krejsa, P. Janas, I. Yilmaz, M. Marschalko, T. Bouchal, The use of the direct optimized probabilistic calculation method in design of bolt reinforcement for underground and mining workings, *The Scientific World Journal*, Article number 267593, 2013.

- [21] Z. Gürdal, R. T. Haftka, P. Hajela, *Design and Optimization of Laminated Composite Material*, J. Wiley & Sons, 1999.
- [22] A. M. Valuev, Models and methods of multiobjective optimization in problems of quarry design and planning, *WSEAS Trans. on Math.*, 13, p. 557-566, 2014.
- [23] E.A. Vorontsova, A projective separating plane method with additional clipping for non-smooth optimization, *WSEAS Trans. on Math.*, 13, p. 115-121, 2014.
- [24] J. Lovíšek, J. Králik, Optimal Control for Elasto-Orthotropic Plate, *Contr. and Cyber. 2*, p. 219-278, 2006.
- [25] http://file.scirp.org/Html/1-4900125_27735.htm
- [26] <https://www.researchgate.net/publication/261218848>